ACS OMEGA

Open Access

http://pubs.acs.org/journal/acsodf

Article

Noninvasive Monitoring of Early Cardiac Fibrosis in Diabetic Mice by [^{68}Ga]Ga-DOTA-FAPI-04 PET/CT Imaging

Kaibin Lin,[#] Dai Shi,[#] Ai Wang, Junbo Ge, Dengfeng Cheng,[*] and Yan Yan[*]

Cite This: *ACS Omega* 2024, 9, 17195−17203

Read Online

ACCESS | Metrics & More | Article Recommendations | Supporting Information

ABSTRACT: Cardiac fibrosis represents one of the representative pathological characteristics in the diabetic heart. Active fibroblasts play an essential role in the progression of cardiac fibrosis. The technologies for noninvasive monitoring of activated fibroblasts still have to be investigated. The purpose of this study was to evaluate the feasibility of targeted fibroblast activation protein (FAP) molecular imaging in the early evaluation of diabetic cardiac fibrosis using [^{68}Ga]Ga-DOTA-FAPI-04 PET/CT. PET/CT imaging was conducted in db/db mice and db/m mice at weeks 12 and 24. Diabetic heart injury was determined using echocardiography and serum biomarkers. Additionally, the levels of cardiac fibrosis were also assessed. In our study, conventional diagnostic modalities, including echocardiography and serum biomarkers, failed to monitor early-stage cardiac dysfunction and fibrosis in diabetic mice. Conversely, the results of [^{68}Ga]Ga-DOTA-FAPI-04 PET/CT imaging demonstrated that diabetic mice had increased myocardial uptake of radioactive tracers in both early-stage and late-stage diabetes, consistent with the elevated FAP expression and increased cardiac fibrosis level. Notably, cardiac PET signals exhibited significant correlations with left ventricular ejection fractions, the E/A ratio, and the level of serum TGF-β1, PIIINP, and sST2. The results demonstrated the potential of [^{68}Ga]Ga-DOTA-FAPI-04 PET/CT imaging for visualizing activated fibroblasts and detecting early-stage diabetic heart injury and fibrosis noninvasively. They also demonstrated the clinical superiority of [^{68}Ga]Ga-DOTA-FAPI-04 PET/CT imaging over echocardiography and serum biomarkers in the early monitoring of diabetes-related cardiac dysfunction and fibrosis.

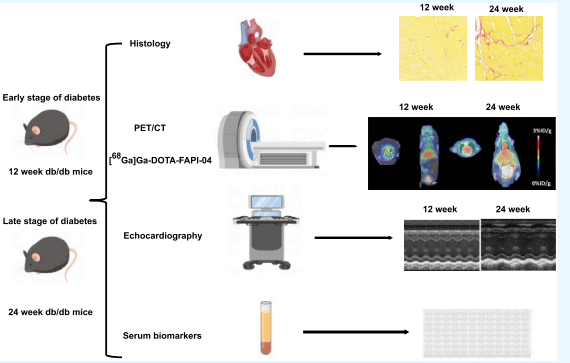

INTRODUCTION

Diabetes mellitus has imposed a substantial burden on global public health, with diabetes-related cardiovascular events accounting for approximately 80% of the diabetes-related deaths.[1] Diabetic cardiomyopathy (DCM) is a type of cardiac injury independent of coronary artery disease or microvascular atherosclerotic disease in diabetic patients.[2] DCM initially manifests as diastolic dysfunction but gradually progresses to systolic dysfunction. Myocardial fibrosis is a representative pathological characteristic of DCM and end-stage heart failure. In diabetic patients, hyperglycemia can induce severe extracellular matrix remodeling, characterized by cardiac fibroblast activation, increased extracellular matrix deposition, impaired collagen dissolution, and myocardial stiffness.[3] The persistence of active fibroblasts and excessive fibrosis significantly impairs cardiac function, thus contributing to poor prognosis in diabetic heart failure.[4] Given the irreversibility and progressive nature of diabetes, effective prevention of diabetes-related cardiovascular complications depends on the early diagnosis of cardiac fibrosis.

At present, cardiac biopsy is the gold standard for the diagnosis of cardiac fibrosis, but its invasiveness limits its usefulness. Therefore, noninvasive monitoring of activated fibroblasts is of great significance for the study of myocardial fibrosis and cardiac remodeling in early-phase diabetes.

Fibroblast activation protein (FAP) is a serine protease selectively expressed on activated stromal fibroblasts. FAP inhibitors (FAPIs) have been developed to detect activated fibroblasts.[5] The FAPI exhibits tremendous potential for assessing pathological cardiac fibrosis, given its low expression in normal physiological hearts.[6]

Most FAPI radiotracers studied to date are labeled with ^{68}Ga for its availability in most PET centers.[7] At present, [^{68}Ga]Ga-DOTA-FAPI-04 has been successfully applied in various cardiovascular diseases, including heart failure,[8] hypertensive heart,[9] pulmonary arterial hypertension,[10] atrial fibrillation,[11] and myocardial infarction.[12] However, few studies have investigated the relationship between the FAP and diabetes-

Received: December 16, 2023
Revised: March 3, 2024
Accepted: March 5, 2024
Published: April 5, 2024

related cardiac fibrosis or applied [^{68}Ga]Ga-DOTA-FAPI-04 PET/CT for assessing diabetes-related cardiac fibrosis.

Therefore, the purpose of this study was to assess the efficacy of [^{68}Ga]Ga-DOTA-FAPI-04 PET/CT imaging in evaluating the degree of cardiac fibrosis in diabetic mice, aiming to provide a theoretical basis for clinical application.

MATERIALS AND METHODS

Animals. All animal procedures were approved by the Animal Care and Use Committee of the Zhongshan Hospital of Fudan University (Shanghai, China). The use and care of animals were in accordance with the Guide for the Care and Use of Laboratory Animals.

C57BLKS/J-LepR (db/db) mice with genetic type 2 diabetes and healthy control mice (db/m) were purchased from GemPharmatech (Nanjing, China). All mice were housed at constant room temperature with daylight from 6 a.m. to 6 p.m. To evaluate the utility of [^{68}Ga]Ga-DOTA-FAPI-04 in early- and late-stage diabetic heart, PET/CT imaging was performed in the mice at the 12 week and the 24 week. Echocardiography images were acquired in all mice before being sacrificed. Tissue samples were collected for subsequent studies. The experimental timeline is illustrated in Figure 1.

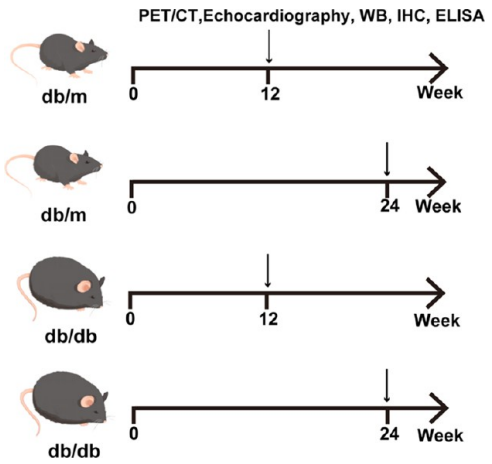

Figure 1. Flowchart of the experimental protocol. WB, Western blot; IHC, immunohistochemistry; and ELISA, enzyme-linked immunosorbent assay.

Echocardiographic Measurement. Mice were kept in light anesthesia with the inhalation of isoflurane (2.5% for induction and 1.5% for maintenance) via a nose cone. Meanwhile, they were fixed on a 37 °C constant-temperature operation table. Transthoracic echocardiography was recorded using Vevo2100 echocardiography system (VisualSonics, Toronto, Canada). Parameters were obtained from more than three beats and then averaged.

Radiopharmaceutical. To radiolabel DOTA-FAPI-04 with $^{68}Ga^{3+}$, 1 mL of 0.25 M sodium acetate and 2 mL of $^{68}Ga^{3+}$ solution (370 MBq in 0.05 M HCl) were added to 100 μg of DOTA-FAPI-04. The reaction mixture was heated to 95 °C for 10 min at pH 4.0. The [^{68}Ga]Ga-DOTA-FAPI-04 was then diluted with normal saline and sterilized through a 0.22 μm Millipore filter using a sterile syringe. The radiochemical purity of [^{68}Ga]Ga-FAPI-04 was higher than 98% as observed by Radio-HPLC.

PET/CT Imaging. Mice were anesthetized with pentobarbital sodium injection and intravenously injected with 100 μL of 3.7 MBq [^{68}Ga]Ga-DOTA-FAPI-04 per mouse. PET/CT (Inveon, Siemens, Germany) scanning protocol was performed immediately after [^{68}Ga]Ga-DOTA-FAPI-04 injection. CT scanning was undertaken with the following setting: tube voltage, 120 kV; tube current, 100 mA; pitch, 1.2; and reconstructed layer thickness, 3.0 mm. CT was used for the attenuation correction and imaging fusion. The region of interest (ROI) of the lesion with obvious radioactivity accumulation in the heart was delineated for the quantification of tracer uptake. Background ROIs with similar diameters were drawn in the area of the right thigh muscle. %ID/g and uptake intensity (target-to-background ratio, TBRs) were calculated within the ROI of the heart.

Western Blot Analysis. Myocardial tissue was lysed in RIPA buffer and quantified with a BCA kit (Thermo, Scientific). A total of 20 μg of proteins was loaded onto SDS-PAGE gels and transferred to the poly(vinylidene fluoride) (PVDF) membrane (Millipore, NY). After blocking in 5% BSA for 1 h at room temperature, the membrane underwent overnight incubation with primary antibodies at 4 °C. The antibodies used in this study were as follows: β-actin (proteintech, 1:5000), FAP (abcam, 1:4000), and α-SMA (abclonal, 1:1000). The immune complexes were detected using a horseradish peroxidase-conjugated secondary antibody and visualized with an enhanced chemiluminescence reagent (Thermo). Signal intensity was quantified in ImageJ and normalized to β-actin.

Quantitative Real-Time Polymerase Chain Reaction (qPCR). Total RNA isolated from tissues was extracted with the TRIzol reagent (15596018, Invitrogen) and reverse-transcribed to cDNA using M-MLV reverse transcriptase (Promega) with random hexamer primers. The mRNA level of the target gene was evaluated by quantitative PCR using SYBR Green Mix (Roche) and an ABI Prism 7900 sequence detection system. The primer sequences used in our study are provided in Table S1.

Histological Analysis and Immunohistochemistry Staining. After PET/CT and echocardiography examinations, the mice were anesthetized with 6 3−4% isoflurane and sacrificed via cervical dislocation. Heart tissues were fixed with 4% paraformaldehyde (PFA) for 24 h and embedded with paraffin or OCT for the paraffin section and frozen section. The paraffin slides of hearts were dissected into 5 μm slices for H&E, Masson's trichrome, Sirius red, and immunohistochemistry. HE staining was used to assess the morphological changes of the hearts. Masson's trichrome and Picrosirius red were performed to evaluate the fibrosis degree. For immunohistochemistry staining (IHC), consecutive 4 μm sections were deparaffinized with xylene and rehydrated in graded alcohols. Circles were drawn by an immunohistochemical pen to prevent liquid leakage. Tissue sections were blocked in 5% BSA for 1 h at 37 °C. Samples were incubated with antibodies against FAP (abcam, 1:500) at 4 °C overnight. Sections were subsequently treated with goat polyclonal secondary antibody against rabbit IgG (Abcam,1:1000). All sections were counterstained with hematoxylin. The sections were observed in a light microscope (Olympus, Japan). Six images from one section were analyzed for fibrosis area and FAP-positive (FAP^+) areas using ImageJ.

Measurement of CK and LDH. The blood was centrifuged at 5000 rpm for 15 min, and the supernatant of

https://doi.org/10.1021/acsomega.3c10061
ACS Omega 2024, 9, 17195−17203

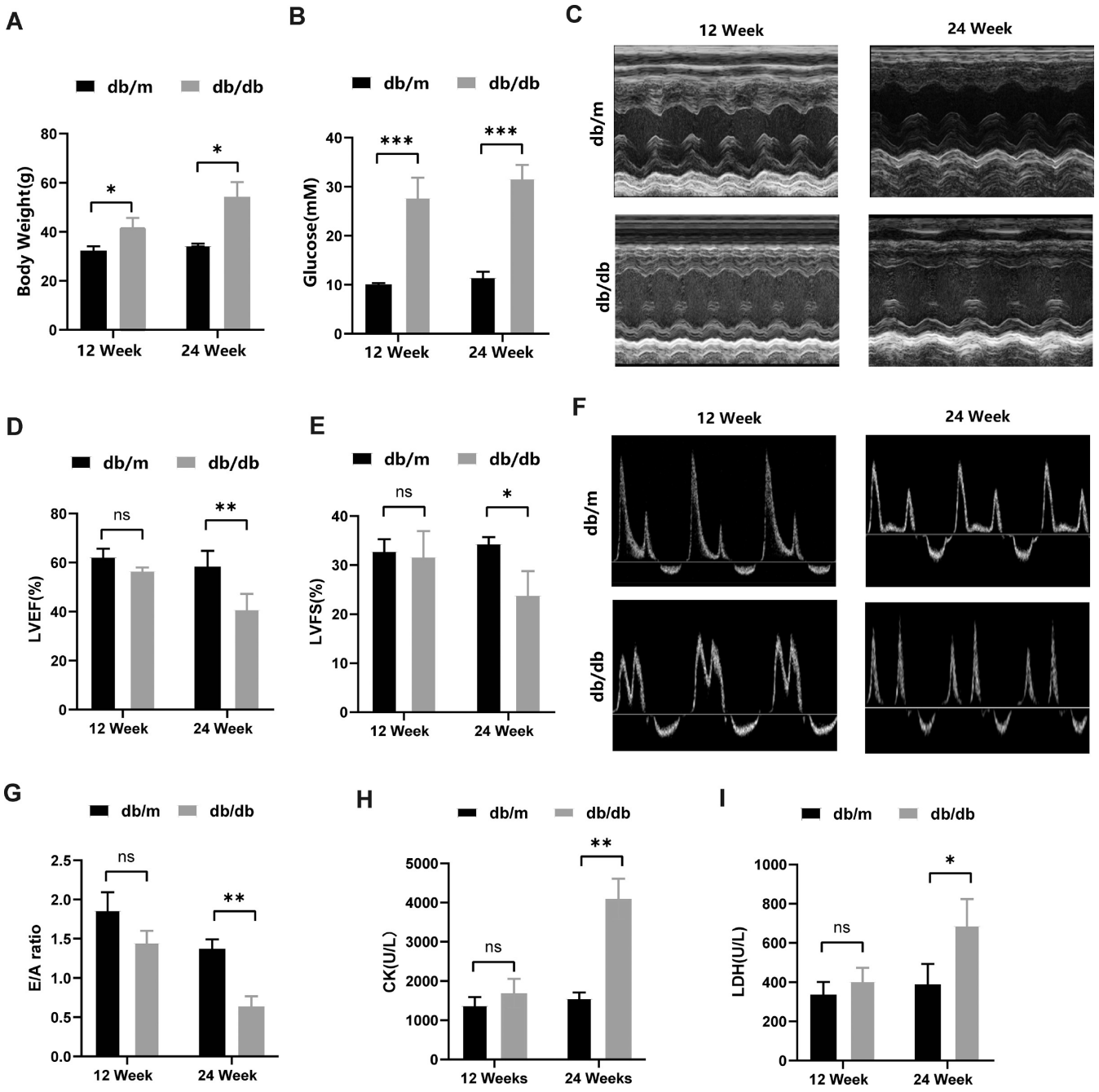

Figure 2. Db/db mice demonstrated cardiac dysfunction in the late-stage diabetes, as evidenced by the results of echocardiography and biomarkers. (A) Body weight. (B) Blood glucose. (C) Representative echocardiograms. (D) Quantification of left ventricular ejection fractions (LVEF). (E) Quantification of left ventricular fractional shortening (LVFS). (F) Representative pulsed-wave Doppler tracings. (G) Quantification of the E/A ratio. (H) Level of serum CK. (I) Level of serum LDH. Data in (A), (B), (D), (E), (G), (H), and (I) were analyzed using Student's *t* test; ns, not significant; $*P < 0.05$; $**P < 0.01$; and $***P < 0.001$.

the serum was used for the experiment. The measurement of creatine kinase (CK) and lactate dehydrogenase (LDH) was through an automatic biochemical analyzer (Siemens Healthcare Diagnostics Inc.) using specific kits (Siemens, Germany).

Enzyme-Linked Immunosorbent Assay (ELISA). In our study, we focused on the classical transforming growth factor (TGF-β1), type III procollagen N-terminal peptide (PIIINP), and soluble ST2 (sST2), which are all related to the progression of cardiac fibrosis and the prognosis of diabetic heart failure.[13−15] The concentration of these fibrosis biomarkers was evaluated by the ELISA kits (Jiangsu Enzymatic immunity, China) according to the manufacturer's instructions. The optical density of each sample was measured by using a microplate reader (Thermo Scientific, USA). The concentration of each sample was measured according to the standard curve.

Statistical Analysis. All results are reported in the form of means ± SD in this study. Comparison between 2 groups was confirmed by the unpaired 2-tailed *t* test. Pearson correlation was computed to evaluate the associations between two continuous variables. The statistical analysis was applied in

https://doi.org/10.1021/acsomega.3c10061
ACS Omega 2024, 9, 17195−17203

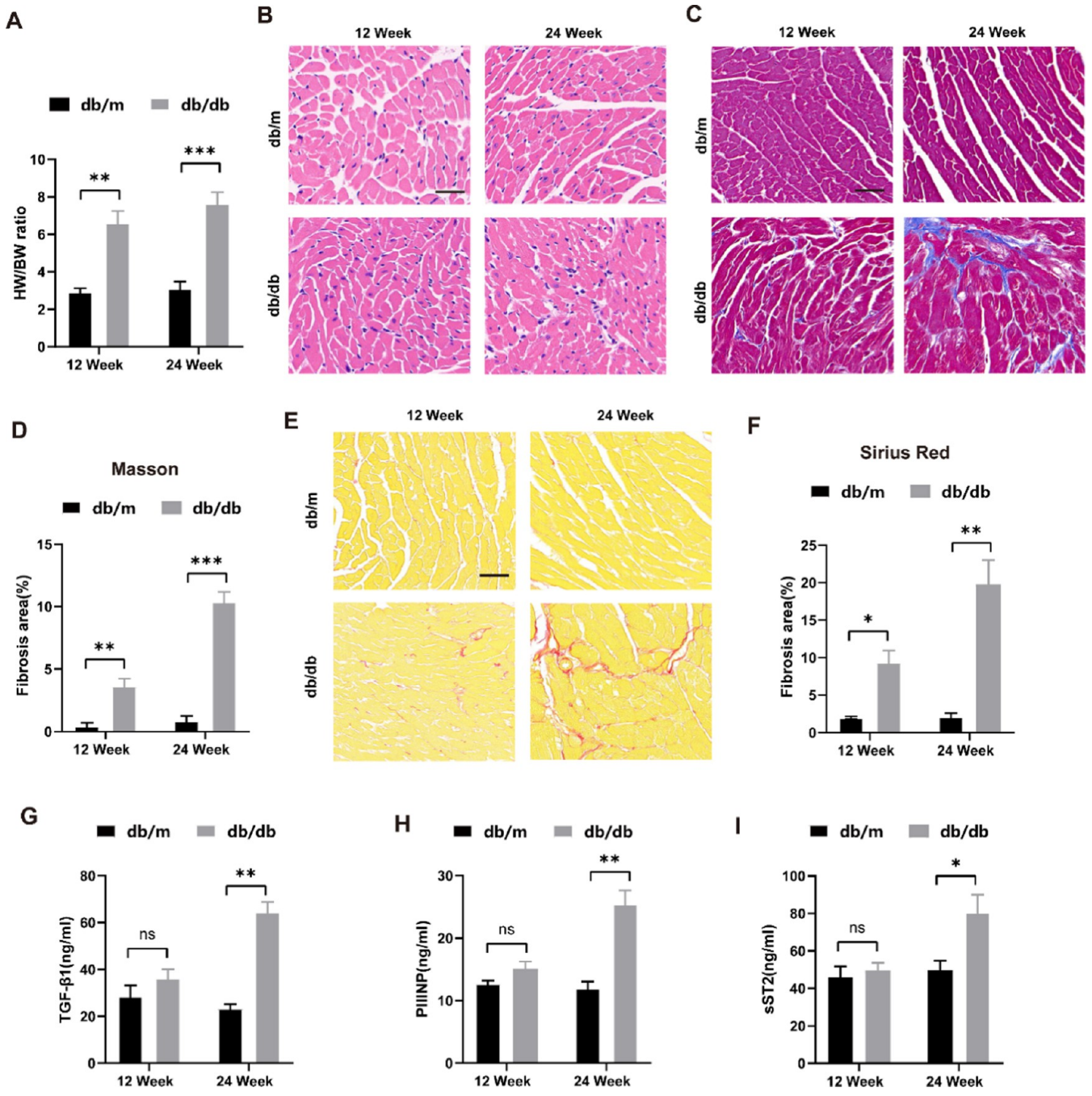

Figure 3. Db/db mice demonstrated cardiac fibrosis in the early- and late-stage diabetes. (A) HW/BW ratio. (B) HE staining. Scale bars, 50 μm. (C, D) Masson staining and quantification of the fibrosis area. Scale bars, 50 μm. (E, F) Sirius red staining and quantification of fibrosis area. Scale bars, 50 μm. (G) Level of serum TGF-β1. (H) Level of serum PIIINP. (I) Level of serum sST2. ns, not significant; data in (A), (D), (F), (G), (H), and (I) were analyzed using Student's t test; *P < 0.05; **P < 0.01; and ***P < 0.001.

GraphPad Pro Prism 8.0 (GraphPad, USA). A statistically significant result was obtained at P value < 0.05.

RESULTS

Diabetes Induces Heart Injury in db/db Mice. The db/db mice at weeks 12 and 24 both exhibited increased body weight (Figure 2A) and blood glucose compared with age-matched db/m mice (Figure 2B). Serial echocardiography was conducted to evaluate the effect of diabetes on cardiac function. Representative left ventricular M-mode echocardiographic images are illustrated in Figure 2C. There were significant differences in cardiac systolic functions between db/db mice and db/m mice at week 24, as evidenced by left ventricular ejection fractions (LVEF) (Figure 2D) and left ventricular fractional shortening (LVFS) (Figure 2E). Meanwhile, left ventricular diastolic function was also monitored (Figure 2F) and the E/A ratio was significantly lower in db/db mice than in db/m mice at week 24 (Figure 2G). Notably, these differences were not observed in comparison of the mice at week 12. Meanwhile, elevated serum CK and LDH were also only observed in the 24 week db/db mice (Figure 2H,I).

Db/db Mice Demonstrated Diabetes-Related Cardiac Remodeling and Fibrosis. Db/db mice exhibited an

https://doi.org/10.1021/acsomega.3c10061
ACS Omega 2024, 9, 17195−17203

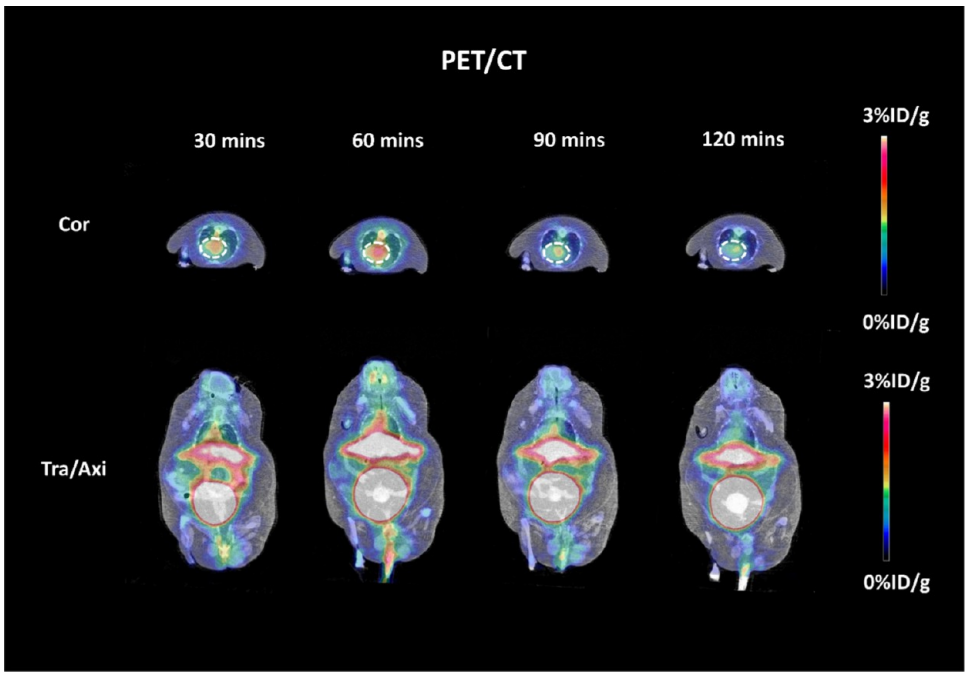

Figure 4. In vivo dynamic imaging of [^{68}Ga]Ga-DOTA-FAPI-04. Representative serial PET/CT images (coronal and axial sections) of a 120 min scan of the db/db group at the 24 week. Hearts are highlighted by a white circle.

increased heart weight (HW)/body weight (BW) ratio (Figure 3A). Histological examination with hematoxylin and eosin (HE) staining revealed severe myocardial disorganization in the 24-week db/db mice but not in the 12-week db/db mice (Figure 3B). Then, we assess the effect of diabetes on cardiac fibrosis. Masson staining (Figure 3C,D) and Sirius red staining (Figure 3E,F) revealed that scattered collagen fibers are distributed in the myocardial interstitial region in both the 12-week and 24-week db/db mice. In order to evaluate the extent of cardiac fibrosis further, we measure the levels of serum TGF-1β, PIIINP, and sST2. Despite the increased levels of serum TGF-1β, PIIINP and sST2 were demonstrated in the 24-week db/db mice, levels of these serum biomarkers remained unchanged in the 12-week db/db mice compared with age-match db/m mice (Figure 3G−I).

Diabetes Induces Diffuse-Activated Cardiac Fibroblast Accumulation Identified by [^{68}Ga]Ga-DOTA-FAPI-04 PET/CT Imaging. A series of dynamic coronal and axial images were captured from 30 to 120 min after tail vein injection of [^{68}Ga]Ga-DOTA-FAPI-04 to identify a time window for optimal imaging of cardiac fibrosis. Rapid tracer distribution to the heart was observed within 30 min, with peak uptake at 60 min followed by a significant decline from 90 to 120 min (Figure 4). The results demonstrated that the diabetic heart had the maximal [^{68}Ga]Ga-DOTA-FAPI-04 uptake at 60 min. Therefore, 60 min was chosen for the following molecular imaging.

As expected, negligible [^{68}Ga]Ga-DOTA-FAPI-04 uptake was discernible in the heart of the 12-week and 24-week db/m mice. However, db/db mice exhibited markedly elevated and widespread myocardial uptake compared with age-matched db/m mice (Figure 5A). Subsequent analyses revealed that [^{68}Ga]Ga-DOTA-FAPI-04 uptake intensity was negatively correlated with both LVEF (Figure 5B) and the E/A ratio, respectively (Figure 5C).

In order to comprehensively assess the potential of [^{68}Ga]Ga-DOTA-FAPI-04 for noninvasive monitoring of cardiac fibrosis, we evaluated the correlation between serum levels of TGF-1β, PIIINP, and sST2 and the intensity of [^{68}Ga]Ga-DOTA-FAPI-04 uptake. The uptake intensity of [^{68}Ga]Ga-DOTA-FAPI-04 was positively correlated with the serum levels of TGF-1β ($P < 0.001$, Figure 5D), PIIINP ($P < 0.001$, Figure 5E), and sST2 ($P < 0.001$, Figure 5F).

FAP Is Upregulated in the Diabetic Heart, Consistent with the Increased mRNA Level of Other Fibrosis Biomarkers. Western blot analysis revealed that higher protein expressions of FAP and α-SMA were detected in the hearts of db/db mice compared with age-match db/m mice (Figure 6A). The results of immunohistochemistry also demonstrated db/db had increased FAP$^+$ area compared with age-match db/m mice (Figure 6B). Additionally, [^{68}Ga]Ga-DOTA-FAPI-04 intensity was positively correlated with the FAP+ area (Figure 6C). The qPCR results also showed that the cardiac mRNA of FAP, collagen I, collagen III, and connective tissue growth factor (CTGF) mRNA were significantly upregulated in both early-stage and late-stage diabetes (Figure 6D−G).

DISCUSSION

In this study, the db/db mice exhibited cardiac dysfunction and increased fibrosis levels in late-stage diabetes, as identified through echocardiography and serum fibrosis biomarkers, respectively. However, they were unable to monitor subtle alterations in early-stage diabetes. Nevertheless, visual observation and quantitative analysis results demonstrated that the FAP-targeted tracer [^{68}Ga]Ga-DOTA-FAPI-04 was significantly concentrated in diabetic heart in both early- and late-stage diabetes, consistent with the expression of FAP. Correlation analysis showed that [^{68}Ga]Ga-DOTA-FAPI-04 uptake was negatively associated with heart function and positively correlated with the levels of serum fibrosis

https://doi.org/10.1021/acsomega.3c10061
ACS Omega 2024, 9, 17195−17203

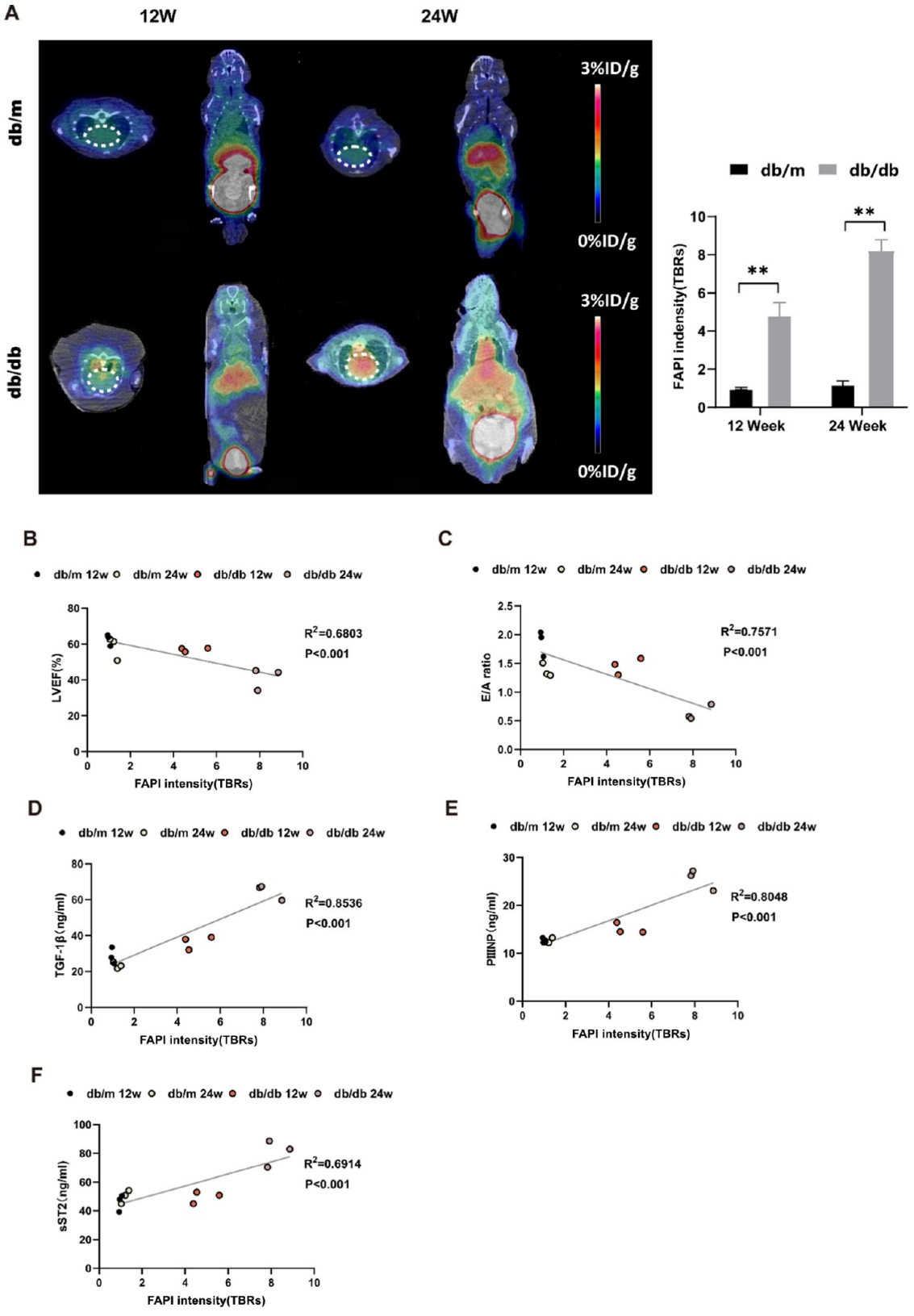

Figure 5. In vivo imaging of [^{68}Ga]Ga-DOTA-FAPI-04 and its correlation with LVEF, E/A ratio, serum TGF-β1, PIIINP, and sST2. (A) Representative PET/CT images of db/db mice and db/m mice at weeks 12 and 24. Hearts are highlighted by a white circle. (B) Correlation between LVEF and [^{68}Ga]Ga-DOTA-FAPI-04PET results. (C) Correlation between the E/A ratio and [^{68}Ga]Ga-DOTA-FAPI-04 PET results. (D) Correlation between the level of serum TGF-β1 and [^{68}Ga]Ga-DOTA-FAPI-04 PET results. (E) Correlation between the level of serum PIIINP and [^{68}Ga]Ga-DOTA-FAPI-04 PET results. (F) Correlation between the level of serum sST2 and [^{68}Ga]Ga-DOTA-FAPI-04 PET results. Data in (A) were analyzed using Student's *t* test; data in (B), (C), (D), (E), and (F) were analyzed using Pearson correlation; ns, not significant; *P < 0.05; **P < 0.01; and ***P < 0.001.

https://doi.org/10.1021/acsomega.3c10061
ACS Omega 2024, 9, 17195−17203

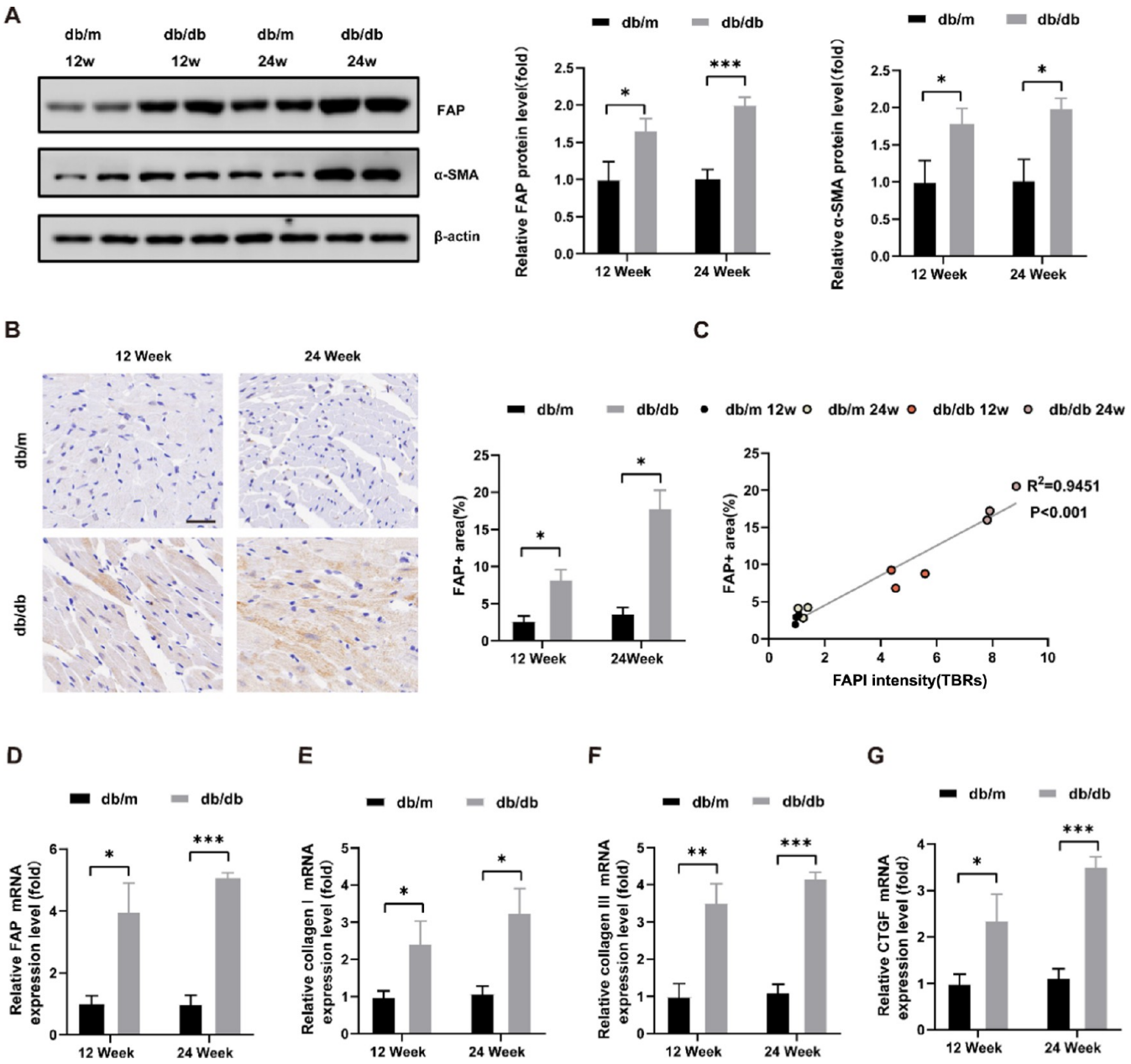

Figure 6. Validation of FAP expression and the mRNA level of fibrosis biomarkers. (A) Representative Western immunoblot images and quantification of α-SMA and FAP. (B) Representative IHC images and quantification for FAP$^+$ area. Scale bar: 50 μm. (C) Correlation between FAP IHC results and [^{68}Ga]Ga-DOTA-FAPI-04 PET results. (D−G) Relative mRNA expression of FAP, collagen I, collagen III, and CTGF. Data in (A), (B), (D), (E), (F), and (G) were analyzed using Student's *t* test; data in (C) were analyzed using Pearson correlation; ns, not significant; *P < 0.05; **P < 0.01; and ***P < 0.001.

biomarkers. These findings effectively demonstrated the clinical potential of [^{68}Ga]Ga-DOTA-FAPI-04 for evaluating the degree of cardiac fibrosis in both early- and late-stage diabetes.

Cardiac remodeling is defined as one of the significant determinants of heart failure progression.[16] In fact, the process of cardiac remodeling involves not only the loss of cardiomyocytes but also the development of fibrosis.[17] Healthy prediabetic patients without concomitant conditions exhibit no significant fibrotic changes.[18] Therefore, exploring noninvasive and sensitive clinical approaches for detecting cardiac fibrosis is essential for the early prevention of diabetic cardiovascular complications.

Cardiac fibrosis is a complex and multifaceted process, with its core characterized by an imbalance between the synthesis and degradation of extracellular matrix proteins, which mediates the abnormal formation and deposition of collagen and leads to the destruction of the myocardial structure and function.[19] Targeting the activation of myofibroblasts from quiescent fibroblasts is an important antifibrotic strategy, but the translation of experimental findings into clinical applications is still limited.

In our study, echocardiography proved to be inept in discerning myocardial impairment during the early phase of diabetes. Additionally, serum fibrosis biomarkers, such as PIIINP, TGF-β1, and sST2, also exhibited circumscribed efficacy in evaluating the magnitude of cardiac fibrosis.

https://doi.org/10.1021/acsomega.3c10061
ACS Omega 2024, 9, 17195−17203

Currently, the prospective utility of FAPI-PET in evaluating nononcologic pathological processes remains under active investigation. A minority of evidence has suggested that FAPI-PET imaging possesses the potential for early identification of cardiovascular fibrosis, risk stratification, and prediction of the progression of left ventricular function.[13]

As expected, our finding substantiated the capability of detecting mild cardiac fibrosis through [^{68}Ga]Ga-DOTA-FAPI-04 molecular imaging. In this study, we found that both FAP protein and mRNA expression were significantly upregulated in the diabetic heart in early- and late-stage diabetes, thereby further affirming the high specificity of the [^{68}Ga]Ga-DOTA-FAPI-04 molecular probe. Notably, [^{68}Ga]Ga-DOTA-FAPI-04 also could monitor the presence of cardiac dysfunction and fibrosis in the early stage, which eluded detection by both echocardiography and serum fibrosis biomarkers. Consequently, [^{68}Ga]Ga-FAPI-04 PET/CT stands poised as a potentially superior diagnostic tool compared to conventional imaging technologies and biomarkers for discerning diabetic heart injury and fibrosis.

However, this study was subject to certain limitations that warrant consideration. First, we did not assess the potential of monitoring cardiac fibrosis in the db/db mice younger than 12 weeks. Meanwhile, while we detected some promising fibrosis biomarkers, these may not comprehensively represent the entire spectrum of possible biomarkers. Finally, the clinical potential of [^{68}Ga]Ga-DOTA-FAPI-04 PET/CT in diabetic patients was not evaluated, and its clinical testing remains pending.

CONCLUSIONS

This study demonstrated that [^{68}Ga]Ga-DOTA-FAPI-04 PET/CT imaging could noninvasively monitor cardiac fibrosis in early-stage diabetes, surpassing the efficacy of both echocardiography and serum biomarkers. Simultaneously, it emerges as a promising diagnostic tool for facilitating early intervention in patients with diabetic heart failure, consequently improving their prognostic outcomes.

ASSOCIATED CONTENT

Data Availability Statement

All datasets generated in this study are included in the article.

Supporting Information

The Supporting Information is available free of charge at https://pubs.acs.org/doi/10.1021/acsomega.3c10061.

Primer sequences used in this study (PDF)

AUTHOR INFORMATION

Corresponding Authors

Dengfeng Cheng − *Department of Nuclear Medicine, Zhongshan Hospital, Institute of Nuclear Medicine, and Cancer Prevention and Treatment Center, Zhongshan Hospital, Fudan University, Shanghai 200032, China; Shanghai Institute of Medical Imaging, Shanghai 200032, China;* orcid.org/0000-0003-2886-3273; Email: cheng.dengfeng@zs-hospital.sh.cn

Yan Yan − *Department of Cardiology, Shanghai Institute of Cardiovascular Diseases, Zhongshan Hospital, Fudan University, Shanghai 200032, China;* orcid.org/0000-0002-1332-9097; Email: yan.yan@zs-hospital.sh.cn

Authors

Kaibin Lin − *Department of Cardiology, Shanghai Institute of Cardiovascular Diseases, Zhongshan Hospital, Fudan University, Shanghai 200032, China*

Dai Shi − *Department of Nuclear Medicine, Zhongshan Hospital, Institute of Nuclear Medicine, and Cancer Prevention and Treatment Center, Zhongshan Hospital, Fudan University, Shanghai 200032, China; Shanghai Institute of Medical Imaging, Shanghai 200032, China;* orcid.org/0000-0003-3903-5713

Ai Wang − *Department of Cardiology, Shanghai Institute of Cardiovascular Diseases, Zhongshan Hospital, Fudan University, Shanghai 200032, China*

Junbo Ge − *Department of Cardiology, Shanghai Institute of Cardiovascular Diseases, Zhongshan Hospital, Fudan University, Shanghai 200032, China*

Complete contact information is available at: https://pubs.acs.org/10.1021/acsomega.3c10061

Author Contributions

#K.L. and D.S. contributed equally to this work. (I) Conception and design: Y.Y., D.C., and J.G.; (II) animal experiments and article writing: K.L. and D.S.; (III) probe synthesis: D.S.; (IV) data analysis and interpretation: K.L., D.S., and A.W.; and (V) final approval of the article: K.L., D.S., A.W., J.G., D.C., and Y.Y.

Funding

This work was financially supported by the National Natural Science Foundation of China (82070463 and 82172002), the Shanghai Municipal Science and Technology Committee of Shanghai outstanding academic leaders plan (21XD1423500), and the Clinical Research Project of Zhongshan Hospital (2020ZSLC20).

Notes

The authors declare no competing financial interest.

ACKNOWLEDGMENTS

The authors thank Figdraw (https://www.figdraw.com) for providing the images of the article.

REFERENCES

(1) Tancredi, M.; Rosengren, A.; Svensson, A. M.; Kosiborod, M.; Pivodic, A.; Gudbjörnsdottir, S.; Wedel, H.; Clements, M.; Dahlqvist, S.; Lind, M. Excess Mortality among Persons with Type 2 Diabetes. *N. Engl. J. Med.* **2015**, *373* (18), 1720−1732.

(2) Sattar, N.; McMurray, J.; Borén, J.; Rawshani, A.; Omerovic, E.; Berg, N.; Halminen, J.; Skoglund, K.; Eliasson, B.; Gerstein, H. C.; McGuire, D. K.; Bhatt, D.; Rawshani, A. Twenty Years of Cardiovascular Complications and Risk Factors in Patients With Type 2 Diabetes: A Nationwide Swedish Cohort Study. *Circulation* **2023**, *147* (25), 1872−1886.

(3) Kenny, H. C.; Abel, E. D. Heart Failure in Type 2 Diabetes Mellitus. *Circ. Res.* **2019**, *124* (1), 121−141.

(4) Salvador, D. B., Jr.; Gamba, M. R.; Gonzalez-Jaramillo, N.; Gonzalez-Jaramillo, V.; Raguindin, P. F. N.; Minder, B.; Gräni, C.; Wilhelm, M.; Stettler, C.; Doria, A.; Franco, O. H.; Muka, T.; Bano, A. Diabetes and Myocardial Fibrosis: A Systematic Review and Meta-Analysis. *JACC Cardiovasc. Imaging* **2022**, *15* (5), 796−808.

(5) Altmann, A.; Haberkorn, U.; Siveke, J. The Latest Developments in Imaging of Fibroblast Activation Protein. *J. Nucl. Med.* **2021**, *62* (2), 160−167.

(6) Aghajanian, H.; Kimura, T.; Rurik, J. G.; Hancock, A. S.; Leibowitz, M. S.; Li, L.; Scholler, J.; Monslow, J.; Lo, A.; Han, W.; Wang, T.; Bedi, K.; Morley, M. P.; Linares Saldana, R. A.; Bolar, N.

A.; McDaid, K.; Assenmacher, C. A.; Smith, C. L.; Wirth, D.; June, C. H.; Margulies, K. B.; Jain, R.; Puré, E.; Albelda, S. M.; Epstein, J. A. Targeting cardiac fibrosis with engineered T cells. *Nature* **2019**, *573* (7774), 430−433.
(7) Li, M.; Younis, M. H.; Zhang, Y.; Cai, W.; Lan, X. Clinical summary of fibroblast activation protein inhibitor-based radiopharmaceuticals: cancer and beyond. *Eur. J. Nucl. Med. Mol. Imaging* **2022**, *49* (8), 2844−2868.
(8) Wang, G.; Yang, Q.; Wu, S.; Xu, X.; Li, X.; Liang, S.; Pan, G.; Zuo, C.; Zhao, X.; Cheng, C.; Liu, S. Molecular imaging of fibroblast activity in pressure overload heart failure using [(68) Ga]Ga-FAPI-04 PET/CT. *Eur. J. Nucl. Med. Mol. Imaging* **2023**, *50* (2), 465−474.
(9) Xie, B.; Li, L.; Lin, M.; Nanna, M.; Su, Y.; Hua, C.; Leng, C.; Gan, Q.; Xi, X. Y.; Wang, Y.; Yao, D.; Wang, L.; Yu, L.; Zhao, L.; Zhang, Y. P.; Dou, K.; Su, P.; Lv, X.; Jia, B.; Yang, M. F. 99mTc-HFAPi imaging identifies early myocardial fibrosis in the hypertensive heart. *J. Hypertens.* **2023**, *41* (10), 1645−1652.
(10) Wang, L.; Zhang, Z.; Zhao, Z.; Yan, C.; Fang, W. (68)Ga-FAPI right heart uptake in a patient with idiopathic pulmonary arterial hypertension. *J. Nucl. Cardiol.* **2022**, *29* (3), 1475−1477.
(11) Li, L.; Gao, J.; Chen, B. X.; Liu, X.; Shi, L.; Wang, Y.; Wang, L.; Wang, Y.; Su, P.; Yang, M. F.; Xie, B. Fibroblast activation protein imaging in atrial fibrillation: a proof-of-concept study. *J. Nucl. Cardiol* **2023**, *30*, 2712−2720, DOI: 10.1007/s12350-023-03352-x.
(12) Zhang, M.; Quan, W.; Zhu, T.; Feng, S.; Huang, X.; Meng, H.; Du, R.; Zhu, Z.; Qu, X.; Li, P.; Cui, Y.; Shi, K.; Yan, X.; Zhang, R.; Li, B. [(68)Ga]Ga-DOTA-FAPI-04 PET/MR in patients with acute myocardial infarction: potential role of predicting left ventricular remodeling. *Eur. J. Nucl. Med. Mol. Imaging* **2023**, *50* (3), 839−848.
(13) Barton, A. K.; Tzolos, E.; Bing, R.; Singh, T.; Weber, W.; Schwaiger, M.; Varasteh, Z.; Slart, R.; Newby, D. E.; Dweck, M. R. Emerging molecular imaging targets and tools for myocardial fibrosis detection. *Eur. Heart J.: Cardiovasc. Imaging* **2023**, *24* (3), 261−275.
(14) Bayes-Genis, A.; de Antonio, M.; Vila, J.; Peñafiel, J.; Galán, A.; Barallat, J.; Zamora, E.; Urrutia, A.; Lupón, J. Head-to-head comparison of 2 myocardial fibrosis biomarkers for long-term heart failure risk stratification: ST2 versus galectin-3. *J. Am. Coll. Cardiol.* **2014**, *63* (2), 158−166.
(15) Frangogiannis, N. G. Transforming growth factor-β in myocardial disease. *Nat. Rev. Cardiol.* **2022**, *19* (7), 435−455.
(16) Azevedo, P. S.; Polegato, B. F.; Minicucci, M. F.; Paiva, S. A. R.; Zornoff, L. A. M. Cardiac Remodeling: Concepts, Clinical Impact, Pathophysiological Mechanisms and Pharmacologic Treatment. *Arq. Bras. Cardiol.* **2016**, *106*, 62−69, DOI: 10.5935/abc.20160005.
(17) Talman, V.; Ruskoaho, H. Cardiac fibrosis in myocardial infarction-from repair and remodeling to regeneration. *Cell Tissue Res.* **2016**, *365* (3), 563−581.
(18) Storz, C.; Hetterich, H.; Lorbeer, R.; Heber, S. D.; Schafnitzel, A.; Patscheider, H.; Auweter, S.; Zitzelsberger, T.; Rathmann, W.; Nikolaou, K.; Reiser, M.; Schlett, C. L.; von Knobelsdorff-Brenkenhoff, F.; Peters, A.; Schulz-Menger, J.; Bamberg, F. Myocardial tissue characterization by contrast-enhanced cardiac magnetic resonance imaging in subjects with prediabetes, diabetes, and normal controls with preserved ejection fraction from the general population. *Eur. Heart J.: Cardiovasc. Imaging* **2018**, *19* (6), 701−708.
(19) Tuleta, I.; Frangogiannis, N. G. Fibrosis of the diabetic heart: Clinical significance, molecular mechanisms, and therapeutic opportunities. *Adv. Drug Delivery Rev.* **2021**, *176*, No. 113904.

https://doi.org/10.1021/acsomega.3c10061
ACS Omega 2024, 9, 17195−17203